Geology, Geophysics & Environment 2025, vol. 51 (1): 71–88

An empirical analysis of changes in the Błędów Desert using machine learning methods

Anna Czernik[1], Natalia Borowiec[2], Urszula Marmol[3]

[1] *Municipal Office of Zakopane, Zakopane, Poland, e-mail: annaczernik@interia.pl, ORCID ID: 0009-0006-7545-9950*
[2] *AGH University of Krakow, Faculty of Geo-Data Science, Geodesy, and Environmental Engineering, Krakow, Poland, e-mail: nboro@agh.edu.pl (corresponding author), ORCID ID: 0000-0001-6051-4300*
[3] *AGH University of Krakow, Faculty of Geo-Data Science, Geodesy, and Environmental Engineering, Krakow, Poland, e-mail: entice@agh.edu.pl, ORCID ID: 0000-0001-8646-7901*

Received: 2 August 2024; accepted: 14 February 2025; first published online: 24 March 2025

Abstract: The aim of the study was to determine changes in the land cover of the Błędów Desert, which is a habitat for rare flora and fauna species protected under the Natura 2000 program. Invasive plants, which pose a threat to protected species, are present in this area. Additionally, human activities can have negative impacts on the desert ecosystem. Therefore, the land manager is obligated to carry out actions aimed at maintaining the appropriate size and character of the desert. The analysis was conducted using satellite imagery from the Sentinel-2 mission, which provides images with high temporal and spatial resolution. The study covered the years 2015–2022 and took into account seasonal variability due to the presence of green vegetation. Change detection methods based on data integration, including photointerpretation and machine learning classification, were used for land cover analysis. Five representative land cover classes were defined, enabling a quantitative presentation of changes in the Błędów Desert and a qualitative assessment of the classification performed. The results of the study indicate variability in land cover depending on the season, with an increasing number of protected plant species, including grasslands. Simultaneously, a slight increase in the desert area was noted, manifesting as an increase in sand in forested areas. The results obtained demonstrate the effective implementation of the Natura 2000 program objectives.

Keywords: desert, machine learning, classification; remote sensing

INTRODUCTION

Change detection in the natural environment using machine learning methods and satellite imagery has become a key tool in ecosystem monitoring worldwide. The development of satellite technologies and machine learning algorithms has enabled data analysis with unprecedented accuracy and detail. Methods such as random forest, support vector machines (SVM), or neural networks, including deep neural networks, are commonly used for land cover classification and change analysis. For example, in the article (Furberg et al. 2020) used SVM to monitor changes in urban green spaces, which allowed for the accurate identification of vegetation loss due to urbanization. A 2016 article, on the other hand, used random forest to classify forest types, making it possible to identify varieties of tree species from satellite imagery (Belgiu & Drăgu 2016).

The use of multispectral satellite imagery, such as that provided by the Sentinel-2 and Landsat

missions, allows the collection of data in different spectral ranges, which is crucial for identifying subtle differences in land cover. Machine learning algorithms, with their ability to process large amounts of data, are an ideal tool for analyzing these images, enabling automatic change detection and classification of different types of coverage. For example, Mountrakis et al. (2011) reviewed the machine learning methods used to analyse satellite images, highlighting their effectiveness in monitoring changes in natural and urban landscapes.

Change detection using machine learning methods is particularly important in the context of global climate change and human activities that affect biodiversity and ecosystem stability. Through accurate temporal analyses, it is not only possible to understand current changes, but also to forecast future trends and threats. In the article (Li et al. 2023) discusses the application of machine learning algorithms, including SVM and random forest, to monitor land cover changes in the context of urban heat islands and climate change. Another article (Zennaro et al. 2021) explores the use of machine learning in climate change risk assessment, highlighting the benefits of integrating remote sensing data for monitoring and forecasting change.

Recent advances in deep learning and machine learning have significantly enhanced the efficacy of forest classification tasks. However, challenges such as limited model variance and restricted generalization capabilities persist, as highlighted in the literature. This study aims to improve classification accuracy by developing a hybrid model that integrates deep learning techniques (specifically ResNet50) and machine learning algorithms (particularly XGBoost), demonstrating that this ensemble approach outperforms individual methods like ResNet50, random forest and light gradient boost machine (Kwenda et al. 2023).

The application of machine learning methods in change detection using satellite imagery represents a significant step forward in environmental research. These methods not only offer high accuracy and precision, but also the possibility of large-scale analysis, which is crucial for global environmental monitoring. The article (Chen et al. 2022) confirms the effectiveness of these methods for urban areas. With the development of satellite technology and algorithms, these methods are expected to play an increasingly important role in natural resource management and conservation.

STUDY AREA: BŁĘDÓW DESERT

The Błędów Desert is located in the eastern part of the Silesian Upland, between the villages of Chechło, Klucze, Laski, Rudy, and Błędów (Fig. 1A). Małopolskie Province contains 86.4% of the desert area, with the remainder located in the Śląskie Province. The total area of the Błędów Desert is 1963.9 ha and constitutes the largest accumulation of sand and gravel areas in Poland. Although it is not a true desert in terms of climate, which is similar to that of the adjacent areas, the name of the area comes from its characteristic landscape (Fig. 1B).

The creation of the desert was the result of anthropogenic factors such as the felling of trees, which exposed sands carried by glacial waters – a natural factor. Mining activities further contributed to the lowering of groundwater levels, thus inhibiting vegetation growth. In the mid-20th century, the area was ploughed and sown, and dust from nearby industrial plants fertilised the soil. Increased water levels, caused by the creation of artificial farm ponds near the desert, also contributed to the growth of vegetation in the sandy areas (Rahmonov 2001).

The desert area consists of two parts: the northern and the southern, separated by the valley of the Biała Przemsza River (Fig. 2). The northern part is entirely within a military complex, while the southern part is managed by the Municipality of Klucze and the City of Dąbrowa Górnicza. The two parts differ in terms of terrain morphology; the northern area is flat and the southern area is more varied. To the north and south of the desert, the land is covered with pine forest (Rahmonow 1999).

The Błędów Desert is included in the list of Natura 2000 sites (PLH1200014 Pustynia Błędowska) by virtue of the European Union Commission Decision of 13 November 2007 (Commission Decision 2008/25/EC). The area is protected for its rare and protected species of flora and fauna. It contains four natural habitats: inland dunes with sand grasslands; warm temperate inland sand turf, a priority natural habitat type; fertile beech forests, found only in the eastern part of the

desert on the Czubatka Hill; willow, poplar, alder and ash forests, occurring in the valley of the Biała Przemsza River (Regionalna Dyrekcja Ochrony Środowiska w Krakowie 2023).

The Błędów Desert is facing several serious threats, which include the covering of sandstone sites by alien species that compete with native flora, which can lead to a reduction in biodiversity.

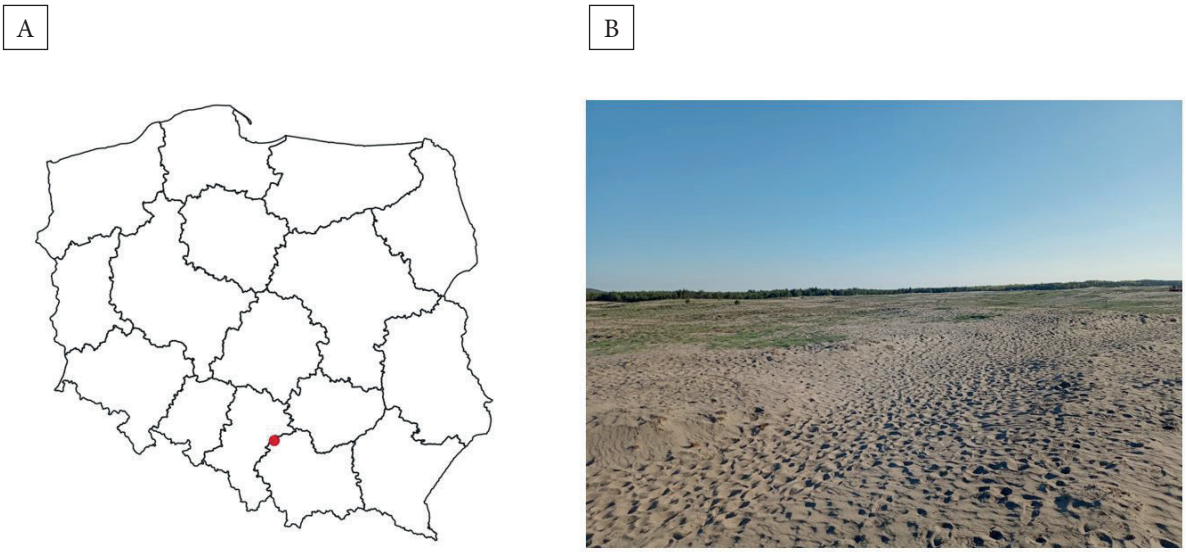

Fig. 1. *Location of the Błędów Desert on a map of Poland (A) and current view (B)*

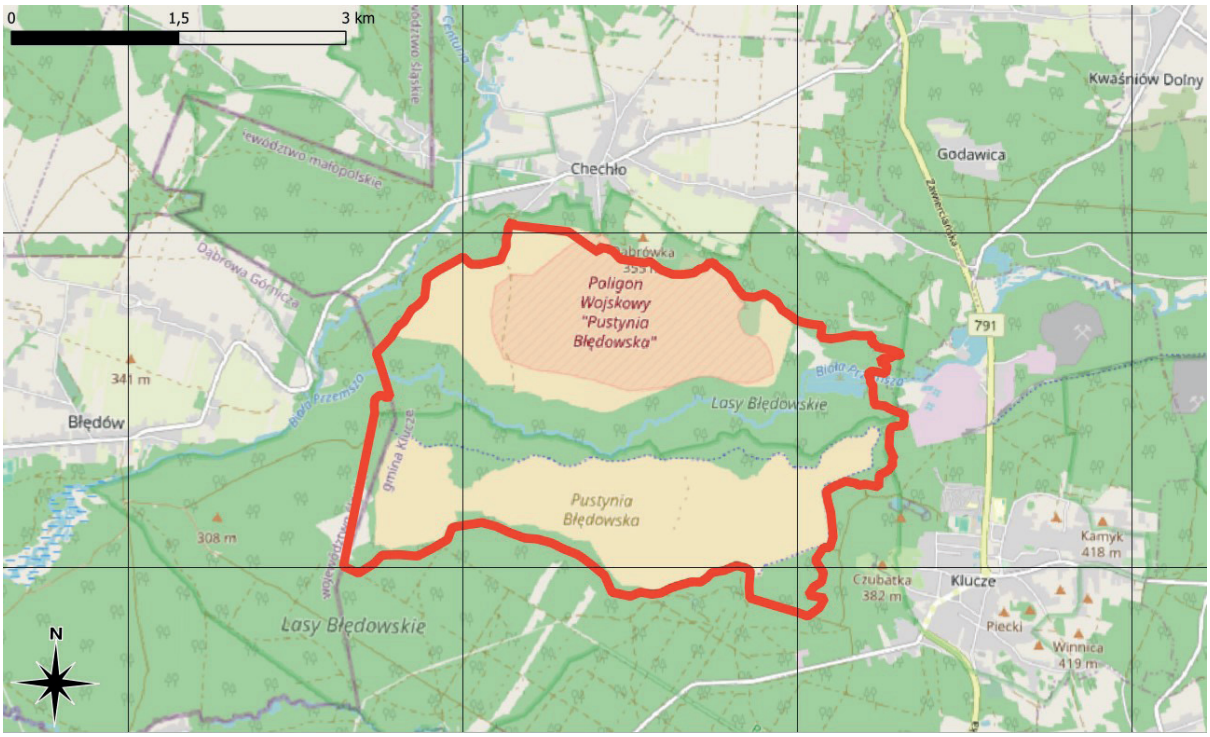

Fig. 2. *Contour of the analysis area (red line) against the background of the Open Street Map*

Acidification of the soil, a process that negatively affects soil conditions, making it difficult for typical plants in the area to survive. Motor vehicle use in habitat areas, motor vehicle traffic destroys soil structure and vegetation, contributing to habitat degradation. Waste impacts, environmental pollution from waste poses a serious threat to the health of the ecosystem (Regionalna Dyrekcja Ochrony Środowiska w Krakowie 2023).

In response to these threats, the present study was conducted to investigate land cover changes in the Błędów Desert over the years. The aim of the research was to analyse the dynamics of habitat changes in detail, to identify the main factors influencing these changes and to assess the effectiveness of conservation measures aimed at preserving the unique natural values of the area. The research provides the basis for formulating recommendations for further conservation and management measures in the Błędów Desert.

DATA USED IN THE RESEARCH

Sentinel satellite imagery was used in the present study. Sentinel-2 was launched under the Copernicus programme, initiated by the European Commission and the European Space Agency (EOS Data Analytics 2024).

The land cover change detection analysis was carried out for the years 2015–2022. The consecutive years were divided into quarters that corresponded to the respective seasons: spring, summer, autumn, and winter. In addition, dates in the corresponding months for each season were selected (spring – March, summer – June, autumn – September, winter – December). Twenty-four Sentinel-2 L2A images with a spatial resolution of 10 m were acquired for the study. The database of acquired data is not 100% full (Table 1). Most of the imagery is missing from 2018, but the imagery acquired from 2019 to 2022 already constitutes a complete input data set.

The missing images in selected periods were due to high cloud cover or their unavailability. Some of the acquired imagery was not used in the study due to overexposure or other interferences negatively affecting the analyses. As a result, three images were removed. Ultimately, the database contained 21 images (Fig. 3). The largest number of missing data was recorded in the fourth quarter. No analyses were carried out during the winter season from 2015 to 2018.

Table 1
Timelines of selected Sentinel-2 L2A data for analysis

Year	Quarter	Month	Day	Year	Quarter	Month	Day
2015	I	–	–	2019	I	March	24
	II	–	–		II	June	9
	III	September	13		III	September	22
	IV	–	–		IV	December	11
2016	I	–	–	2020	I	March	28
	II	June	29		II	June	13
	III	September	27		III	September	21
	IV	December	16		IV	December	15
2017	I	March	29	2021	I	March	3
	II	May	31		II	June	21
	III	–	–		III	September	9
	IV	December	26		IV	November	25
2018	I	–	–	2022	I	March	28
	II	June	7		II	June	26
	III	–	–		III	August	27
	IV	–	–		IV	January	4

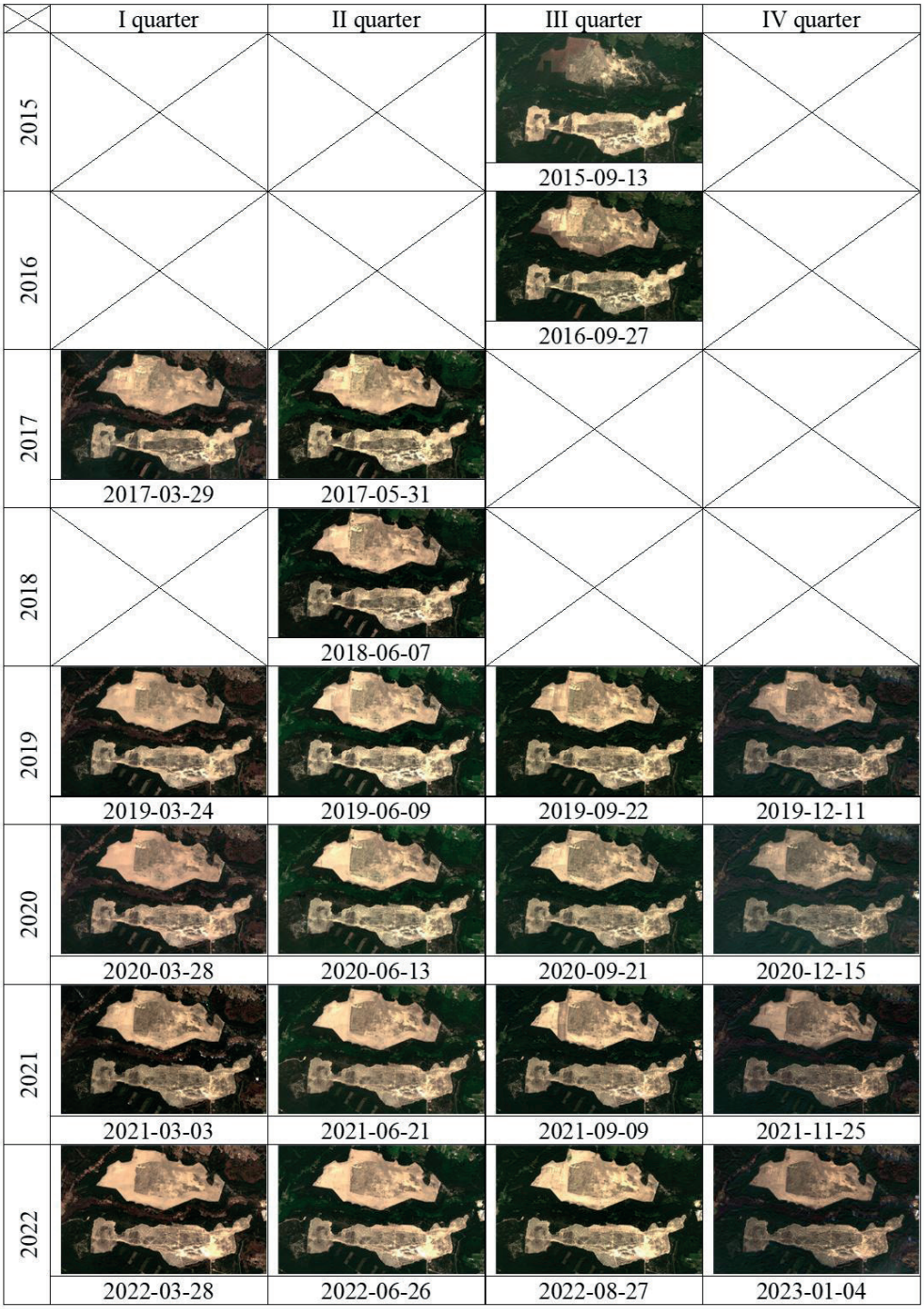

Fig. 3. *RGB color compositions on which analyses were performed*

RESEARCH CHARACTERISTICS

In order to better illustrate and facilitate understanding of the conducted research, below is a flowchart that graphically shows all of the stages of data processing employed (Fig. 4). This diagram provides a holistic view of the research process, allowing a better understanding of the relationships between the various steps. Later in the article, each of these steps is described in detail, including the methods used, the tools employed, and the results obtained.

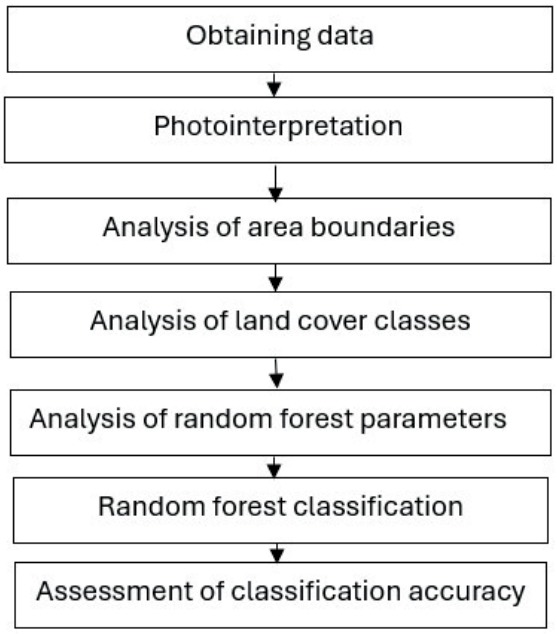

Fig. 4. *The diagram of the next stages of the research*

The research began with the photointerpretation of satellite images to identify land cover types and changes over time. Photointerpretation involved the visual analysis of satellite images, allowing for the identification of various types of land cover and their changes over the years. During this stage, satellite images were processed and analysed for colours, textures, and patterns characteristic of different types of land cover. This made it possible to distinguish five characteristic classes in the study area:

1) sand – yellow pixel, indicating sand-covered terrain;
2) forest – dark green pixel, indicating areas covered with high vegetation;
3) bare soil – dark brown pixel, indicating land not covered by vegetation;
4) grasslands – light green pixel, indicating areas covered with low vegetation;
5) turf – light brown pixel, indicating areas within the sand class that do not exhibit features of bare soil or meadow classes.

Although the Biała Przemsza River flows through the middle of the Błędów Desert, the decision was made not to distinguish a water class. The reason for this was the width of the watercourse, which is about 2–3 m in the field. Working with images that have a ground pixel resolution of 10 m would not allow for the clear distinction of this class in this area.

The bare soil class was only analysed in images from the first and fourth quarters, while the meadow class was analysed in images from the second and third quarters. This was due to the absence of these types of land cover in all the time periods taken for analysis.

The study used random forest classification, a machine learning method that employs a set of decision trees to perform classification. This is a non-parametric machine learning algorithm based on constructing decision trees. In each node, random training fields (bootstrap) are selected, which eliminates overfitting and results in the algorithm's resistance to noise (Mishina et al. 2015).

Random forest classification is a technique that requires the precise selection of two key parameters: number of training samples and number of trees. In the context of this study, the default value for the number of training samples is 5000, meaning that the regions of interest did not exceed 5000 pixels. The second key parameter is the number of decision trees, which directly affects the accuracy of the model. A smaller number of trees leads to lower model accuracy, but reduces the computation time. Due to the importance of this parameter in assessing classification accuracy, tests were carried out to optimize it. Based on research (Van Anh et al. 2021) an experiment was conducted, testing different values of decision trees. In this study, the number of trees set to 500 (ntree = 500) gave satisfactory results, achieving an overall accuracy (OA) above 90% and a kappa coefficient above 0.90 (Table 2). Overall accuracy is a measure that shows the percentage of correctly classified samples relative to the entire dataset. The kappa coefficient, on the other hand, is a more sophisticated measure of classification consistency that takes into account random imputations.

Table 2
Results of classification accuracy tests for different values of the tree number parameter

Model parameter	**13.09.2015**		**27.09.2016**		**29.03.2017**	
ntree	300	500	300	500	300	500
OA [%]	84.5	96.1	86.9	93.7	94.0	92.9
Kappa coefficient	0.79	0.94	0.81	0.90	0.92	0.90

Based on the above tests, classification was performed on each dataset, assigning pixels to the corresponding land cover classes. The classification algorithm was based on supervised machine learning methods, where the model was previously trained on a known dataset and then applied to classify new images. After the classification of each dataset, an accuracy assessment was performed, which is a key element in verifying the results. The classification accuracy assessment process involved several steps. The first was the generation of an error matrix (confusion matrix) for each image. The confusion matrix is a tool that represents the numbers of correctly and incorrectly classified pixels for each class. It is an essential element in verifying classification accuracy, allowing detailed analysis of the results (Marmol & Borowiec 2023). From this matrix, accuracy assessment metrics such as overall classification accuracy (ACC), accuracy per class (precision, recall), and weighted average (F1 score) were calculated. These results were presented in tabular and graphical form to identify trends and potential problems in classification.

RESULTS AND ANALYSIS

In this section, the classification results of the satellite images are discussed in detail, paying particular attention to the accuracy assessment achieved with the error matrix analysis and the classification quality indicators used.

Classification analysis

The classification was performed on all selected satellite images, with an example of a visual result shown below (Fig. 5). The land cover classification results are presented in tables, divided into quarters, which allowed for the tracking of seasonal changes. Each table contains percentage and area values for the five representative land cover classes (Chapter "Research characteristics"). The percentage share of each class indicates the proportion of the area covered, while the area values are given in hectares. The average values for each class were obtained by averaging the results from each quarter, which allows for the visualization of long-term trends in land cover changes. This analysis enabled the identification of seasonal patterns, such as an increase in vegetation in spring and summer and a decrease in autumn and winter. These results are crucial for understanding the dynamics of changes in the Błędów Desert ecosystem and the effectiveness of conservation measures. Additionally, for each quarter, charts were drawn to visualize the percentage share of each class in the respective time periods (Figs. 6–9).

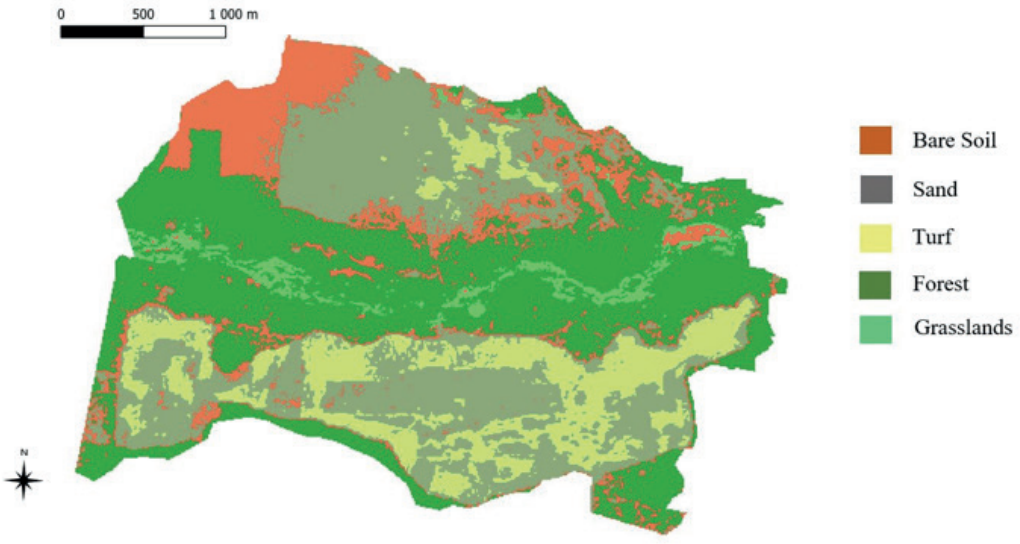

Fig. 5. *An example of a classification result using the random forest method*

Quarter I

Tables 3 and 4 show average land cover class values of: sand 26.2% (301.3 ha), turf 38.1% (438.2 ha), forest 25.1% (289.3 ha), bare soil 10.5% (121.4 ha). The overall accuracy of the classification ranges from 94.3 to 98.6% with an average value of 96.6%. This is a very good result. The kappa coefficient maintains an average level of 0.95. Over the years, it ranges from 0.92 to 0.98, which indicates an excellent agreement (McHugh 2012).

Analysing the above results (Fig. 6), the following conclusions can be drawn. The curve representing turf is very dynamic – it does not maintain a constant level, nevertheless it has an increasing trend.

Table 3
Land cover change detection results for Quarter I in percentage terms

Classification results	2017-03	2019-03	2020-03	2021-03	2022-03	Mean
Sand [%]	27.2	30.8	27.3	18.4	27.3	26.2
Turf [%]	37.0	32.6	36.1	46.6	38.2	38.1
Forest [%]	25.7	24.2	24.8	25.6	25.4	25.1
Bare soil [%]	10.1	12.5	11.7	9.4	9.1	10.5
Grassland [%]	–	–	–	–	–	–
Overall accuracy [%]	98.6	97.2	94.3	95.3	97.5	96.6
Kappa coefficient	0.98	0.96	0.92	0.93	0.96	0.95

Table 4
Detection results of land cover changes for Quarter I by area

Land cover area	2017-03	2019-03	2020-03	2021-03	2022-03	Mean
Sand [ha]	313.3	354.3	313.8	211.2	313.8	301.3
Turf [ha]	425.7	374.6	415.2	535.9	439.5	438.2
Forest [ha]	295.8	278.4	285.1	295.0	292.4	289.3
Bare soli [ha]	115.7	143.4	134.2	108.5	105.0	121.4
Grassland [ha]	–	–	–	–	–	–

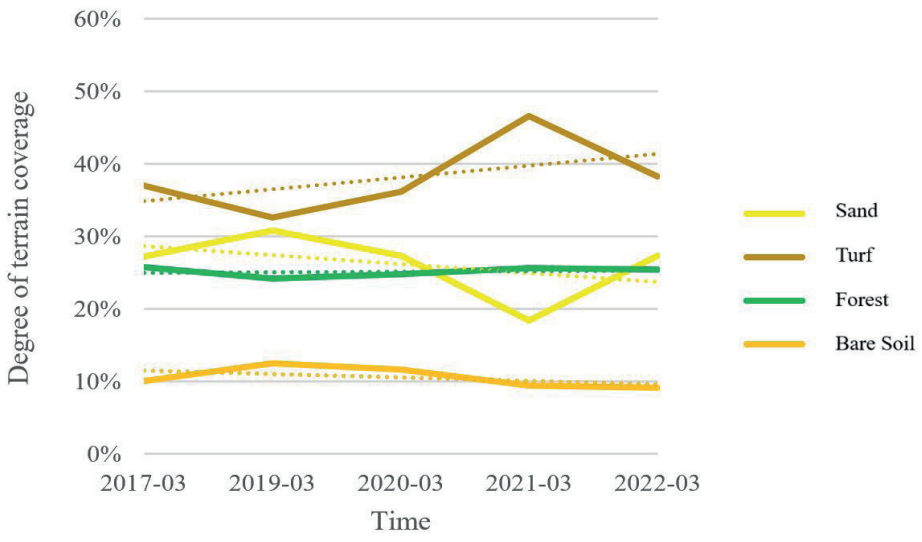

Fig. 6. *Detection results of land cover changes for Quarter I by class (dotted lines – trend of individual land cover class)*

Over the years, the turf area has occupied the Błędów Desert to the greatest extent. The difference in land cover between the minimum value (2019) and the maximum value (2021) is 14.0 percentage points and this translates into 161.3 ha. The graph for sand is the reverse of the curve for turf with the land cover trend reversed. The difference between the minimum (2021) and maximum (2019) proportion of land cover is 12.4 percentage points (143.0 ha). The curves for forest and bare soil are stable. The forest area, unlike the bare soil, tends to increase gently. Over the years, forest has covered the Błędów Desert to a similar extent. The discrepancy between the extreme values is 1.5 percentage points (17.4 ha) and the situation is analogous for the bare soil class. The difference of 3.3 percentage points translates into 38.3 ha. Uncovered soil consistently records the lowest land cover in the first quarter of each year.

Quarter II

In Tables 5 and 6, the average land cover values in Quarter II over the six years are: sand 24.7% (283.6 ha), turf 39.7% (456.8 ha), forest 28.3% (325.5 ha), grassland 7.4% (84.7 ha). During the Quarter II periods, bare soil was not analysed. The overall accuracy remains at 90.9% with the lowest quotation of 89.6% occurring in 2020 and the highest of 91.8% obtained in 2018. The kappa coefficient values over the years in Quarter II are 0.85 and 0.88 with an average score of 0.87. A stabilization of the index can be observed.

Figure 7 shows that there is a downward trend in the turf curve. It reached its minimum in 2019, amounting to 36.1% of land cover, which translates into 415.0 ha. It reached its highest value in 2017, where it was 46.1% (529.9 ha). The difference is 10 percentage points (114.9 ha). As of 2019, the average value of the turf class has reached 37.5% (431.2 ha). The land cover of sand was increasing rapidly until 2019. Over the two years, the value increased by 10 percentage points (115.4 ha). Thereafter, it fell gently until 2021, when it reached an extreme of 24.7%, or 284.0 ha. It then increased by 2.9 percentage points to a value of 27.6% (317.2 ha) of land cover. The curve for the forest is very stable. The difference between the extreme values over the years is 1.9 percentage points (22.1 ha). There is an upward trend. The graph for grassland, as for forest, is stabilised. The difference between 2017, when the maximum land cover was reached, and 2022, when the minimum was reached, is 1.1 percentage points, or 12.2 ha. The curve maintains a gentle downward trend.

Table 5
Land cover change detection results for Quarter II in percentage terms

Classification results	2017-05	2018-06	2019-06	2020-06	2021-06	2022-06	Mean
Sand [%]	18.8	21.9	28.9	26.1	24.7	27.6	24.7
Turf [%]	46.1	42.2	36.1	38.1	39.0	36.7	39.7
Forest [%]	27.1	28.4	27.8	28.5	29.1	28.8	28.3
Bare soil [%]	–	–	–	–	–	–	–
Grassland [%]	8.0	7.4	7.3	7.3	7.3	6.9	7.4
Overall accuracy [%]	90.7	91.8	90.2	89.6	91.2	91.7	90.9
Kappa coefficient	0.86	0.88	0.86	0.85	0.87	0.88	0.87

Table 6
Detection results of land cover changes for Quarter II by area

Land cover area	2017-05	2018-06	2019-06	2020-06	2021-06	2022-06	Mean
Sand [ha]	216.5	252.1	331.9	300.1	284.0	317.2	283.6
Turf [ha]	529.9	485.9	415.0	438.7	448.7	422.4	456.8
Forest [ha]	312.3	327.2	320.0	327.8	334.3	331.5	325.5
Bare soil [ha]	–	–	–	–	–	–	–
Grassland [ha]	91.8	85.5	83.8	84.0	83.4	79.6	84.7

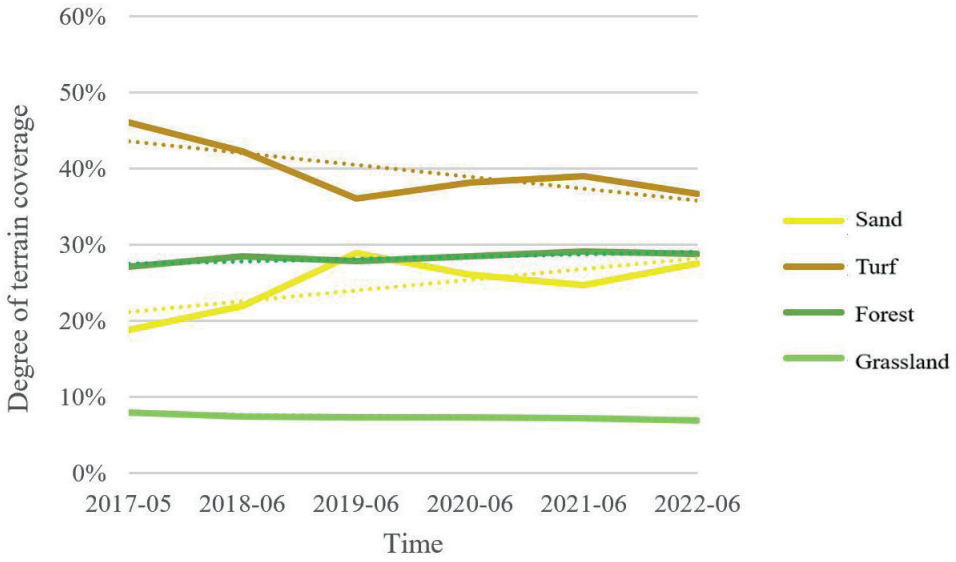

Fig. 7. *Detection results of land cover changes for Quarter II by class (dotted lines – trend of individual land cover class)*

Quarter III

Over the six years studied, Quarter III land cover averages: sand 15.2% (174.6 ha), turf 44.7% (514.1 ha), forest 33.1% (380.6 ha), grassland 4.2% (48.8 ha) (Tables 7, 8). The overall accuracy varies between 92.5–97.2%. The average is 94.6%. It reached a maximum in 2019 and a minimum in 2021. The kappa coefficient is unstable and is between 0.88–0.96, with an average value of 0.92.

Table 7
Land cover change detection results for Quarter III in percentage terms

Classification results	2015-09	2016-09	2019-09	2020-09	2021-09	2022-08	Mean
Sand [%]	13.8	11.5	18.1	18.7	9.6	19.3	15.2
Turf [%]	31.4	48.0	45.3	44.9	54.3	44.2	44.7
Forest [%]	38.6	32.7	32.0	32.1	32.1	31.1	33.1
Grassland [%]	2.5	4.5	4.6	4.4	4.1	5.4	4.2
Bare soil [%]	13.6	3.3	–	–	–	–	–
Overall accuracy [%]	96.0	93.7	97.2	93.1	92.5	94.7	94.6
Kappa coefficient	0.94	0.90	0.96	0.90	0.88	0.92	0.92

Table 8
Detection results of land cover changes for Quarter III by area

Land cover area	2015-09	2016-09	2019-09	2020-09	2021-09	2022-08	Mean
Sand [ha]	159.2	132.5	208.7	214.7	110.2	222.3	174.6
Turf [ha]	361.7	552.6	521.0	516.6	624.2	508.3	514.1
Forest [ha]	443.8	375.9	368.4	369.1	368.9	357.6	380.6
Grassland [ha]	28.9	51.9	52.4	50.2	47.3	62.4	48.8
Bare soli [ha]	156.9	37.5	–	–	–	–	–

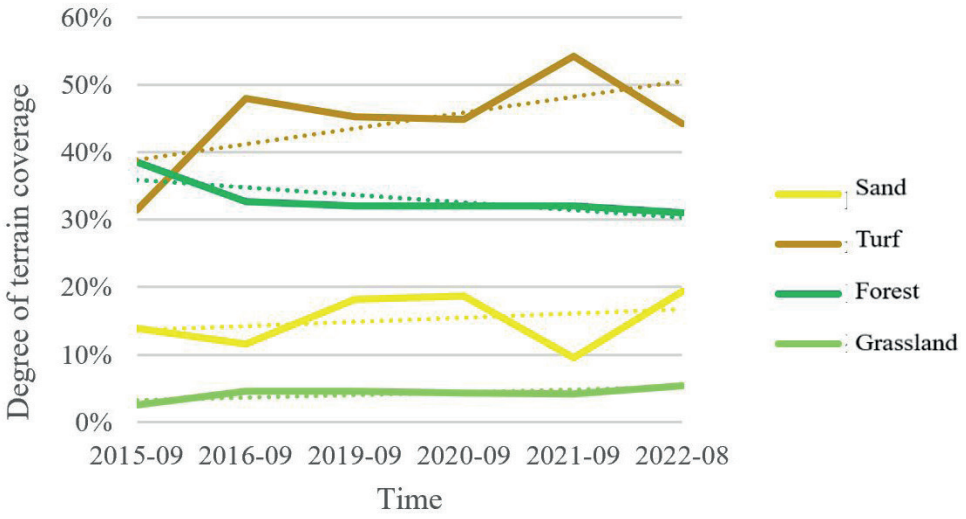

Fig. 8. *Detection results of land cover changes for Quarter III by class (dotted lines – trend of individual land cover class)*

Analysing Figure 8, it can be stated that the land cover values for turf over the years are inconsistent; however, the trend is upward. During the first year of the study, the indicator increased by 16.6 percentage points to 48.0% (552.6 ha). It then declined to 44.9% (516.6 ha) by 2020. The following year, it sharply rose by 9.4 percentage points, and in 2022 it returned to a level close to that of two years prior, at 44.2%, or 508.3 ha. The difference between the extreme values (2015 and 2021) is 22.8 percentage points, or 262.4 ha.

The sand cover curve is similarly variable to that of the turf class, but the trend is not as rapidly increasing. The difference between the first and second analysed images (2015–2016) is 2.3 percentage points, translating to 26.7 ha. In the years 2019–2020, the cover curve remained at a similar level (18.1% and 18.7%). The following year, the value dropped to 9.6% (110.2 ha), then increased by 9.7 percentage points to 19.3%, or 222.3 ha. The difference between the minimum and maximum values is 9.7 percentage points (112.1 ha), occurring in the images from 2021 to 2022.

The land cover graph for the forest area shows stabilization beyond the first analysed period. The 2015 image had a value of 38.6% (443.8 ha). In subsequent years, it remained at an average level of 32.0% (368.0 ha). The higher forest cover in 2015 was due to deforestation in the northern part of the Błędów Desert in later years. A downward trend is observed. The difference between the extreme values (2015 and 2022) is 7.5 percentage points, or 86.2 ha.

The meadow curve shows a slight upward trend. The difference between the extremes is 2.9 percentage points, or 33.5 ha. The highest level, 5.4%, was reached in 2022, covering 62.4 ha.

Quarter IV

For Quarter IV, the average land cover is: sand 17.3% (198.9 ha), turf 45.2% (519.9 ha), forest 28.8% (331.4 ha), bare soil 8.7% (100.3 ha) (Tables 9, 10). The curves for all classes are very stable. The total accuracy reaches an average of 92.9% (min. 91.8%, max. 93.5%) and the kappa coefficient 0.89 (the lowest value obtains 0.88, the highest value 0.90).

Figure 9 shows that the proportion of land cover by turf varies between 43.9% and 46.7%. It reaches its maximum value in 2021, where it reaches 537.4 ha, and its minimum value in 2023 (505.4 ha). The difference is 2.8 percentage points. This translates into 32.0 ha. Both of these values had information taken from photographs with a staggered date relative to the previous ones. In 2021, the images are from November, while the data for Quarter IV 2022 were taken from January 2023.

Table 9
Land cover change detection results for Quarter IV in percentage terms

Classification results	2019-12	2020-12	2021-11	2023-01	Mean
Sand [%]	17.1	16.6	15.5	20.0	17.3
Turf [%]	44.9	45.3	46.7	43.9	45.2
Forest [%]	29.0	29.0	29.1	28.2	28.8
Grassland [%]	–	–	–	–	–
Bare soil [%]	9.1	9.2	8.7	7.9	8.7
Overall accuracy [%]	91.8	93.4	93.5	93.0	92.9
Kappa coefficient	0.88	0.90	0.90	0.90	0.89

Table 10
Detection results of land cover changes for Quarter IV by area

Land cover area	2019-12	2020-12	2021-11	2023-01	Mean
Sand [ha]	196.3	191.0	178.3	229.9	198.9
Turf [ha]	516.1	520.7	537.4	505.4	519.9
Forest [ha]	333.4	333.1	335.3	323.9	331.4
Grassland [ha]	–	–	–	–	–
Bare soil [ha]	104.7	105.7	99.5	91.4	100.3

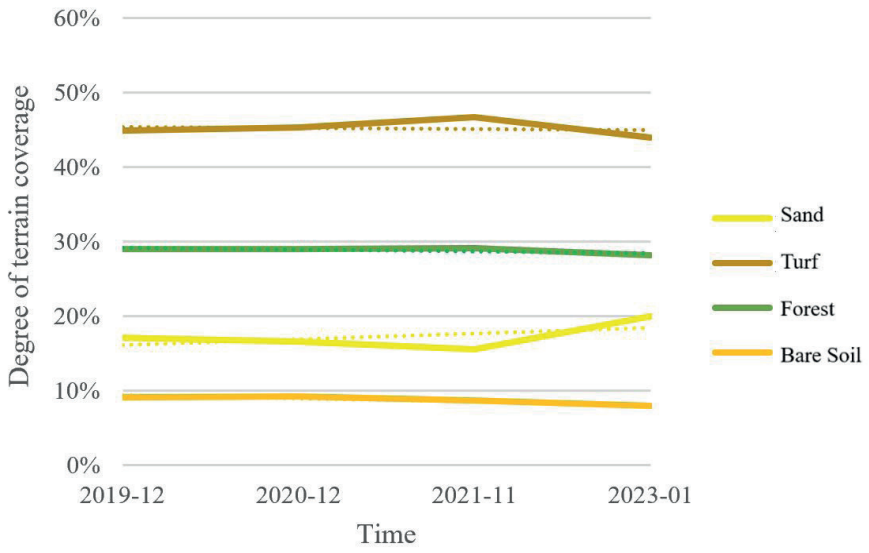

Fig. 9. *Detection results of land cover changes for Quarter IV by class (dotted lines – trend of individual land cover class)*

The shifting of these dates is assumed to cause slight fluctuations in the land cover values of each class. There is a gently decreasing trend. The sand curve gently decreases from a value of 17.1% to a value of 15.5% (178.3 ha) by 2021. This is followed by an increase of 4.5 percentage points, or 51.5 ha. This results in an increasing trend of the sand curve. The difference between the minimum value (2021) and the maximum value (2023) is 4.5 percentage points, or 51.5 ha. The graphs for the forest and bare soil classes show no significant change. For forest, the difference between the extremes is 1 percentage point (11.4 ha) and for bare soil 1.3 percentage points (14.4 ha). As a result of the changes in land cover in the last analysed image for Quarter IV, both curves achieve a slight downward trend.

Error matrix and calculated indices

Image classification was assessed using performance coefficients, which were calculated from an error matrix. The error matrix is a basic tool for assessing the quality of a classification model, allowing the calculation of a number of derived coefficients (Goldblatt et al. 2017, Drobnjak et el. 2019).

In the present study, the following coefficients were calculated (Tables 11–17):

- TPR (true positive rate) – sensitivity, i.e. the proportion of truly positive class relative to all positive cases;
- TNR (true negative rate) – specificity, i.e. the proportion of truly negative class relative to all negative cases;
- PPV (positive predictive value) – the proportion of positive predictions confirmed by a genuinely positive condition;
- NPV (negative predictive value) – the proportion of negative predictions confirmed by a genuinely negative condition;
- ERR (error rate) – the proportion of misclassifications relative to all classifications;
- F1 (F1 score) – the harmonic mean between PPV and TPR, which is a measure of the balance between precision and sensitivity (Das et al. 2021);
- ACC (accuracy) – the proportion of correct classifications relative to all classifications.

TPR index

The true positive rate, which indicates the proportion of correctly classified true positives among all positives, shows considerable variability depending on the class of site and the period of analysis.

For the entire dataset, the TRP index ranges from 0.67 to 1.00, with the maximum value of 1.00 reached in 42% of cases, indicating high classification accuracy. 61% of the results exceeded the value of 0.90, confirming good agreement of the classification models. The highest values were obtained in the third quarters of the analysed years, with the maximum result occurring in 2022. The forest class had high TRP indices, with the best results achieved by the grassland class (average index of 0.94). The lowest value (0.67) was recorded for the grassland class in the second quarter of 2018, but overall, the index remained high. The sand class had an average index of 0.91, and the bare soil class had an index of 0.90. The average TRP index for all classes was 0.92, confirming the high quality of the classification (Table 11).

Table 11
TPR index for the classes in each image

Date	Sand	Turf	Forest	Bare soil	Grass-land
2015-09	0.71	1.00	1.00	–	1.00
2016-09	0.83	0.93	1.00	–	0.80
2017-03	1.00	0.83	1.00	0.86	–
2017-05	1.00	0.86	0.80	–	1.00
2018-06	0.89	0.92	1.00	–	0.67
2019-03	0.91	1.00	0.90	1.00	–
2019-06	1.00	0.83	0.91	–	0.83
2019-09	0.89	1.00	1.00	–	0.83
2019-12	0.86	0.93	1.00	0.71	–
2020-03	0.90	0.83	1.00	1.00	–
2020-06	0.80	1.00	0.82	–	1.00
2020-09	1.00	0.93	0.91	–	0.83
2020-12	0.88	0.93	1.00	0.86	–
2021-03	1.00	0.93	0.90	0.86	–
2021-06	0.80	1.00	0.91	–	0.83
2021-09	1.00	0.88	1.00	–	0.83
2021-11	1.00	1.00	0.82	0.86	–
2022-03	1.00	1.00	0.90	1.00	–
2022-06	1.00	0.92	0.82	–	1.00
2022-08	0.89	0.93	1.00	–	1.00
2023-01	0.78	1.00	0.91	1.00	–

TNR index

The true negative rate, which measures the proportion of correctly classified negative cases, averaged 0.97, with a minimum value of 0.89, indicating very good classification quality. The maximum value of 1.00 was reached in 38% of cases. For the turf class, TNR ranged from 0.89 to 1.00, with an average of 0.96, peaking in 2017 and 2021. For the sand class, TNR ranged from 0.93 to 1.00, with an average of 0.98, showing high consistency across quarters. The forest class had TNR values between 0.93 and 1.00, averaging 0.98, with fluctuations in certain years. The bare soil class showed TNR from 0.97 to 1.00, with an average of 0.98, although lower values were recorded in the first and fourth quarters. The grassland class had the highest TNR, ranging from 0.97 to 1.00, with an average of 0.99 and consistent high values in most quarters (Table 12).

PPV index

The precision of the positive prediction defines the proportion of correctly classified positive cases among all cases classified as positive.

In the surveys conducted, the target PPV of 1.00 was reached in 38% of the cases, and 70% of the results exceeded 0.9, indicating high classification accuracy. The best results were achieved in the fourth quarters, where the majority of images were from 2022, particularly for the grassland class. The bare soil class had the highest PPV of 0.86, with 93% of results close to 1.00. The turf class had the lowest PPV of 0.81, recorded in the second quarters of 2020 and 2021. The average PPV across all surveys was 0.93, indicating strong classification performance. For the sand class, the PPV ranged from 0.83 to 1.00, with an average of 0.93. The forest class had a PPV range from 0.85 to 1.00, with an average of 0.94. The grassland class showed the highest PPV, ranging from 0.83 to 1.00, with an average of 0.97. The highest values for grassland were achieved in 2019, 2021, and 2022. The lowest PPV for sand was recorded in the third quarter of 2016 at 0.83. The forest class showed the lowest PPV in 2018 and 2021, with the highest values achieved in 2019, 2020, and 2022 (Table 13).

NPV index

The negative precision index indicates the percentage of correctly classified negative cases among all cases classified as negative.

The study achieved an NPV of 1.00 in 42% of cases, and all results exceeded 0.9, reflecting high accuracy. The best results were obtained in the first quarters, particularly for the forest class, with the highest levels achieved in 2022. Classes such as sand, bare soil (Quarter IV 2019), and grassland (Quarter II 2018) reached minimum values of 0.94, while the turf class had the lowest minimum value of 0.92 in Quarter III 2021. The overall NPV for the study reached an average of 0.98, indicating excellent prediction quality. The turf class showed values ranging from 0.92 to 1.00, with fluctuations between years, peaking at 1.00 in 2020–2021. The sand class had values between 0.94 and 1.00,

Table 12
TNR index for the classes in each image

Date	Sand	Turf	Forest	Bare soil	Grass-land
2015-09	1.00	0.94	1.00	–	1.00
2016-09	0.97	0.96	0.97	–	1.00
2017-03	0.97	1.00	0.97	0.97	–
2017-05	0.98	0.98	0.98	–	0.97
2018-06	0.97	0.96	0.93	–	1.00
2019-03	1.00	0.96	1.00	0.97	–
2019-06	0.93	0.96	0.97	–	1.00
2019-09	1.00	0.96	0.97	–	1.00
2019-12	0.97	0.92	0.96	1.00	–
2020-03	0.97	0.96	1.00	0.97	–
2020-06	1.00	0.89	1.00	–	0.97
2020-09	0.97	1.00	0.97	–	0.97
2020-12	0.97	0.96	0.97	1.00	–
2021-03	0.97	1.00	0.97	0.97	–
2021-06	1.00	0.89	0.97	–	1.00
2021-09	0.97	1.00	0.93	–	1.00
2021-11	1.00	0.96	0.97	0.97	–
2022-03	1.00	0.96	1.00	1.00	–
2022-06	0.97	0.93	1.00	–	1.00
2022-08	0.97	0.96	1.00	–	1.00
2023-01	1.00	0.93	1.00	0.97	–

Table 13
PPV index for the classes in each image

Date	Sand	Turf	Forest	Bare soil	Grass-land
2015-09	1.00	0.83	1.00	–	1.00
2016-09	0.83	0.93	0.92	–	1.00
2017-03	0.91	1.00	0.91	0.86	–
2017-05	0.89	0.92	0.89	–	0.96
2018-06	0.89	0.92	0.85	–	1.00
2019-03	1.00	0.92	1.00	0.88	–
2019-06	0.85	0.91	0.91	–	1.00
2019-09	1.00	0.93	0.92	–	1.00
2019-12	0.86	0.87	0.92	1.00	–
2020-03	0.90	0.91	1.00	0.88	–
2020-06	1.00	0.81	1.00	–	0.86
2020-09	0.90	1.00	0.91	–	0.83
2020-12	0.88	0.93	0.92	1.00	–
2021-03	0.90	1.00	0.90	0.86	–
2021-06	1.00	0.81	0.91	–	1.00
2021-09	0.88	1.00	0.85	–	1.00
2021-11	1.00	0.93	0.90	0.86	–
2022-03	1.00	0.93	1.00	1.00	–
2022-06	0.92	0.85	1.00	–	1.00
2022-08	0.89	0.93	1.00	–	1.00
2023-01	1.00	0.88	1.00	0.88	–

with notable variations in the second quarter, including a drop to 0.94 in 2020–2021. For the forest class, the NPV ranged from 0.93 to 1.00, with consistent values of 1.00 in some years and a low of 0.94 in 2022. The bare soils class showed values between 0.94 and 1.00, with the lowest values recorded in 2017 and 2021, and the highest in other years. The grasslands class had a range from 0.94 to 1.00, with an average of 0.98; the lowest value of 0.94 was recorded in Quarter II 2018, and it later increased to 1.00 in 2022. The NPV index showed stability in the third trimester, maintaining 1.00 in 2015 and 2022, and 0.97 in other years (Table 14).

F1 index

The F1 index, which is the harmonic average of the True positive rate and positive predictive value, is a key measure of the quality of classifiers. The higher the index value, the better the classification performance.

In the study, a F1 index of 1.00 was achieved in 10% of the cases, with 70% of results exceeding 0.9. The highest F1 values were recorded in the fourth quarters, with 2022 producing five images at 1.00. The best F1 scores were for the grassland class, ranging from 0.87 to 0.97, with the lowest values recorded in Quarter I 2020 and Quarter II 2019. The random forest classifier had the lowest performance for grassland, scoring 0.80 in Quarter II 2018. The turf class achieved an average F1 of 0.92, with 0.87 recorded in Quarter I 2020 and Quarter II 2019. In Quarter I, the F1 index increased from 0.91 in 2017 to 0.96 in 2019, 2021, and 2022, except for 2020, which saw a drop to 0.87. In Quarter II, the F1 values ranged from 0.87 in 2019 to 0.90 in 2020, maintaining this value in 2021, with 0.88 in 2022. In Quarter III, the F1 index grew from 0.91 in 2015 to 0.97 in 2019, decreasing to 0.93 in 2022. The sand class had an F1 range from 0.83 to 1.00, averaging 0.92, with 1.00 achieved in 2022. The forest class showed F1 values between 0.84 and 1.00, averaging 0.93, and reached 1.00 in 2020. The bare soil class had an F1 index between 0.83 and 1.00, with an average of 0.90, and peaked at 1.00 in 2022. The grassland class fluctuated between 0.80 and 1.00, with an average of 0.92, reaching 1.00 in 2022 (Table 15).

Table 14
NPV index for the classes in each image

Date	Sand	Turf	Forest	Bare soil	Grass-land
2015-09	0.94	1.00	1.00	–	1.00
2016-09	0.97	0.96	1.00	–	0.97
2017-03	1.00	0.93	1.00	0.97	–
2017-05	1.00	0.95	0.96	–	1.00
2018-06	0.97	0.96	1.00	–	0.94
2019-03	0.97	1.00	0.97	1.00	–
2019-06	1.00	0.93	0.97	–	0.97
2019-09	0.97	1.00	1.00	–	0.97
2019-12	0.97	0.96	1.00	0.94	–
2020-03	0.97	0.93	1.00	1.00	–
2020-06	0.94	1.00	0.94	–	1.00
2020-09	1.00	0.96	0.97	–	0.97
2020-12	0.97	0.96	1.00	0.97	–
2021-03	1.00	0.96	0.97	0.97	–
2021-06	0.94	1.00	0.97	–	0.97
2021-09	1.00	0.92	1.00	–	0.97
2021-11	1.00	1.00	0.93	0.97	–
2022-03	1.00	1.00	0.97	1.00	–
2022-06	1.00	0.96	0.94	–	1.00
2022-08	0.97	0.96	1.00	–	1.00
2023-01	0.94	1.00	0.97	1.00	–

Table 15
F1 index for the classes in each image

Date	Sand	Turf	Forest	Bare soil	Grass-land
2015-09	0.83	0.91	1.00	–	1.00
2016-09	0.83	0.93	0.96	–	0.89
2017-03	0.95	0.91	0.95	0.86	–
2017-05	0.94	0.89	0.84	–	0.98
2018-06	0.89	0.92	0.92	–	0.80
2019-03	0.95	0.96	0.95	0.93	–
2019-06	0.92	0.87	0.91	–	0.91
2019-09	0.94	0.97	0.96	–	0.91
2019-12	0.86	0.90	0.96	0.83	–
2020-03	0.90	0.87	1.00	0.93	–
2020-06	0.89	0.90	0.90	–	0.92
2020-09	0.95	0.96	0.91	–	0.83
2020-12	0.88	0.93	0.96	0.92	–
2021-03	0.95	0.96	0.90	0.86	–
2021-06	0.89	0.90	0.91	–	0.91
2021-09	0.93	0.93	0.92	–	0.91
2021-11	1.00	0.97	0.86	0.86	–
2022-03	1.00	0.96	0.95	1.00	–
2022-06	0.96	0.88	0.90	–	1.00
2022-08	0.89	0.93	1.00	–	1.00
2023-01	0.88	0.93	0.95	0.93	–

ERR index

The error rate is a measure indicating the number of incorrect classifications in relation to all classifications made. A high ERR value indicates a higher percentage of errors made by the algorithm.

In the study, an ERR value of 0.00 was achieved in 10% of the cases, indicating excellent classification quality. 75% of the results exceeded the average ERR value, demonstrating high compliance. The best results were obtained for the third quarters, with the lowest ERR recorded in four images from this period. Five images from 2022 had the lowest ERR values, with three for the forest class and three for the grassland class. The highest ERR of 0.08 was observed in the grassland class in seven images, while the lowest was 0.03 in six images. The average ERR value was 0.04, ranging from 0.00 to 0.08, which is considered very good. For the grassland class, ERR ranged from 0.03 to 0.08, averaging 0.05. In Quarter I 2017, the ERR was 0.05, dropping to 0.03 in 2019, and reaching its highest value of 0.08 in 2020. From 2021 to 2022, the ERR remained at 0.03. In Quarter II, the ERR was 0.06 in 2017, with a minimum of 0.05 in 2019 and a maximum of 0.08 in 2020–2022. In Quarter III, the ERR ranged from 0.03 to 0.05, with a minimum in 2019–2020. In Quarter IV, ERR decreased from 0.08 in 2019 to 0.03 in 2021, reaching 0.05 in 2023. The sand class had an ERR range of 0.00 to 0.05, with an average of 0.04, reaching 0.00 in 2021–2022. For the forest class, ERR ranged from 0.00 to 0.08, averaging 0.03, with the lowest value in 2020. The bare soil class showed ERR values between 0.00 and 0.05, with an average of 0.03, reaching 0.05 in 2019 and 2021. The grassland class had ERR values between 0.00 and 0.05, with an average of 0.02, decreasing to 0.00 in 2022 (Table 16).

ACC index

The accuracy index, a measure of overall classification accuracy, reports the percentage of correct classifications relative to all classifications made.

The analysis yielded ACC values ranging from 0.92 to 1.00. The maximum level of 1.00 was reached in 10 per cent of cases, demonstrating the very high compliance of the classification algorithm.

Table 16
ERR index for the classes in each image

Date	Sand	Turf	Forest	Bare soil	Grassland
2015-09	0.05	0.05	0.00	–	0.00
2016-09	0.05	0.05	0.02	–	0.02
2017-03	0.03	0.05	0.03	0.05	–
2017-05	0.02	0.06	0.06	–	0.02
2018-06	0.05	0.05	0.05	–	0.05
2019-03	0.03	0.03	0.03	0.03	–
2019-06	0.05	0.08	0.05	–	0.03
2019-09	0.03	0.03	0.03	–	0.03
2019-12	0.05	0.08	0.03	0.05	–
2020-03	0.05	0.08	0.00	0.03	–
2020-06	0.05	0.08	0.05	–	0.03
2020-09	0.03	0.03	0.05	–	0.05
2020-12	0.05	0.05	0.03	0.03	–
2021-03	0.03	0.03	0.05	0.05	–
2021-06	0.05	0.08	0.05	–	0.03
2021-09	0.03	0.05	0.05	–	0.03
2021-11	0.00	0.03	0.08	0.05	–
2022-03	0.00	0.03	0.03	0.00	–
2022-06	0.03	0.08	0.05	–	0.00
2022-08	0.05	0.05	0.00	–	0.00
2023-01	0.05	0.05	0.02	0.02	–

Table 17
ACC index for the classes in each image

Date	Sand	Turf	Forest	Bare soil	Grassland
2015-09	0.95	0.95	1.00	–	1.00
2016-09	0.95	0.95	0.98	–	0.98
2017-03	0.97	0.95	0.97	0.95	–
2017-05	0.98	0.94	0.94	–	0.98
2018-06	0.95	0.95	0.95	–	0.95
2019-03	0.98	0.98	0.98	0.98	–
2019-06	0.95	0.93	0.95	–	0.98
2019-09	0.98	0.98	0.98	–	0.98
2019-12	0.95	0.92	0.97	0.95	–
2020-03	0.95	0.92	1.00	0.97	–
2020-06	0.95	0.93	0.95	–	0.98
2020-09	0.98	0.98	0.95	–	0.95
2020-12	0.95	0.95	0.98	0.98	–
2021-03	0.98	0.98	0.95	0.95	–
2021-06	0.95	0.93	0.95	–	0.98
2021-09	0.98	0.95	0.95	–	0.98
2021-11	1.00	0.98	0.93	0.95	–
2022-03	1.00	0.98	0.98	1.00	–
2022-06	0.98	0.93	0.95	–	1.00
2022-08	0.95	0.95	1.00	–	1.00
2023-01	0.95	0.95	0.98	0.98	–

All other results achieved a value above 0.90, which also confirms the high degree of accuracy. The highest ACC index values were recorded in the third quarters, covering four images, including two from the autumn season of 2022. Two of these images represented the grassland class. The best results were achieved for the sand, bare soil and grassland classes, with a minimum ACC index value of 0.95. These results were obtained for eleven images in the sand class, four images in the bare soil class and two images in the grassland class. The lowest ACC index value of 0.92 was recorded for the grassland class in the first quarter of 2020 and in the fourth quarter of 2019. The average ACC index value for all surveys was 0.96, which is a very good result. A maximum value of 1.00 was obtained in 10% of the cases (Table 17).

The results indicate high classification accuracy for all analysed classes, with the lowest ACC index values observed mainly in some quarters, which may suggest seasonal variations in the data or differences in the quality of the satellite images.

CONCLUSION

The research carried out in the Błędów Desert was aimed at analysing land cover changes from 2015 to 2022 using random forest classification based on Sentinel-2 imagery. The study assumed that this method would allow the detailed determination of changes in the share of different land cover classes and evaluation of the impact of natural and anthropogenic factors on these changes. A key aspect was also the verification of the effectiveness of the random forest classification in the context of remote sensing applications and to compare the results with other studies on the use of Sentinel-2 data.

Solving the research problem included:

- performing Sentinel-2 image classification using the random forest algorithm,
- analysing the dynamics of changes in different land cover classes from year to year,
- evaluating the impact of natural factors (seasonality, temperature changes) and human activities (stand removal) on land cover variability,
- evaluation of classification accuracy and its comparison with other methods.

The results showed that the largest area is occupied by protected turf habitat (41.8%), and the smallest by low vegetation and exposed soil. The share of sand in land cover averaged 20.9%, forest 29.0%, uncovered soil 9.7%, and grassland 5.8%, with their highest share in the second quarter of the year. An important finding was the relationship between sand areas and grassy vegetation – an increase in vegetation cover leads to a decrease in sandy areas.

Verification of classification accuracy showed the high degree of consistency of the results, which was confirmed by performance indicators: the average classification accuracy was 95%, and the kappa coefficient reached a value of at least 0.85. Indicators such as TPR, TNR, PPV, NPV, F1 and ACC had values above 0.80, confirming the high quality of classification, with the highest classification errors for the grassland class.

The analysis carried out demonstrated the effectiveness of random forest classification in monitoring land cover changes in the Błędów Desert based on Sentinel-2 imagery. The method proved effective in detecting changes, especially in the semi-desert environment. The main changes are in sand cover and grass vegetation, which have a dynamic relationship, indicating the process of desert overgrowth. Seasonal factors and temperature influence the dynamics of changes in land cover, with the largest areas of sand observed in spring and forests in autumn. The classification results confirm previous studies on the effectiveness of Sentinel-2 data and the random forest algorithm, according to Forkuor et al. (2018) and Belgiu & Drăgu (2016). Limitations of the analysis are the incompleteness of the database in some periods and the limited spatial resolution (10 m), which may be insufficient for analysing narrow objects, such as watercourses. Despite the high accuracy of the classification, analysis of satellite imagery is not a substitute for field monitoring, which is necessary to accurately distinguish individual habitats. Further studies in future years will allow the observation of long-term trends and identification of new ecological processes occurring in the Błędów Desert.

Funding: The article was prepared under the research subvention of the AGH University of Krakow No. 16.16.150.545 in 2025.

Data Availability Statement: Satellite images on which the research was conducted are available online at https://eos.com/landviewer/ [access: 12.31.2023].

REFERENCES

Belgiu M. & Drăgu L., 2016. Random forest in remote sensing: A review of applications and future directions. *ISPRS Journal of Photogrammetry and Remote Sensing*, 114, 24–31. https://doi.org/10.1016/J.ISPRSJPRS.2016.01.011.

Chen J., Guo Z. & Huang J., 2022. Deep learning of spatio-temporal patterns for urban mobility prediction using big data. *Information Systems Research*, 33(2), 579–598. https://doi.org/10.1287/ISRE.2021.1072.

Commission Decision of 13 November 2007 adopting, pursuant to Council Directive 92/43/EEC, a first updated list of sites of Community importance for the Continental biogeographical region. http://data.europa.eu/eli/dec/2008/25(1)/oj [access: 22.01.2024].

Das C., Sahoo A.K. & Pradhan C., 2021. Multicriteria recommender system using different approaches. [in:] Mishra S., Tripathy H.K., Mallick P.K., Sangaiah A.K. & Chae G.-S. (eds.), *Cognitive Big Data Intelligence with a Metaheuristic Approach*, Academic Press, 153–161. https://doi.org/10.1016/B978-0-323-85117-6.00011-X.

Drobnjak S., Jakovljević G. & Sekulović D., 2019. The possibility of application of remote sensing in managing crisis situations. [in:] Sekulović D. (ed.), *Application of Geographic Information System in Modeling of Natural Catastrophe*, Faculty of Information Technology and Engineering, University "Union-Nikola Tesla", Belgrade, 181–204.

EOS Data Analytics, 2024. *Sentinel-2: Satellite Imagery, Overview, And Characteristics*. https://eos.com/find-satellite/sentinel-2/ [access: 22.01.2024].

Forkuor G., Dimobe K., Serme I. & Tondoh J.E., 2018. Landsat-8 vs. Sentinel-2: Examining the added value of sentinel-2's red-edge bands to land-use and land-cover mapping in Burkina Faso. *GIScience and Remote Sensing*, 55(3), 331–354. https://doi.org/10.1080/15481603.2017.1370169.

Furberg D., Ban Y. & Mörtberg U., 2020. Monitoring urban green infrastructure changes and impact on habitat connectivity using high-resolution satellite data. *Remote Sensing*, 12(18), 3072. https://doi.org/10.3390/RS12183072.

Goldblatt R., Ballesteros A.R. & Burney J., 2017. High spatial resolution visual band imagery outperforms medium resolution spectral imagery for ecosystem assessment in the semi-arid Brazilian Sertão. *Remote Sensing*, 9(12), 1336. https://doi.org/10.3390/RS9121336.

Kwenda C., Gwetu M.V. & Fonou-Dombeu J.V., 2023. Forest image classification based on deep learning and XGBoost algorithm. [in:] Mikyška J., de Mulatier C., Paszynski M., Krzhizhanovskaya V.V., Dongarra J.J., Sloot P.M.A. (eds.), *Computational Science – ICCS 2023: 23rd International Conference, Prague, Czech Republic, July 3–5, 2023, Proceedings, Part IV*, Springer, Cham, 217–229. https://doi.org/10.1007/978-3-031-36027-5_16.

Li F., Yigitcanlar T., Nepal M., Nguyen K. & Dur F., 2023. Machine learning and remote sensing integration for leveraging urban sustainability: A review and framework. *Sustainable Cities and Society*, 96, 104653. https://doi.org/10.1016/J.SCS.2023.104653.

Marmol U. & Borowiec N., 2023. Analysis and verification of building changes based on point clouds from different sources and time periods. *Remote Sensing*, 15(5), 1414. https://doi.org/10.3390/RS15051414.

McHugh M.L., 2012. Interrater reliability: The kappa statistic. *Biochemia Medica*, 22(3), 276–282. https://doi.org/10.11613/BM.2012.031.

Mishina Y., Murata R., Yamauchi Y., Yamashita T. & Fujiyoshi H., 2015. Boosted random forest. *IEICE Transactions on Information and Systems*, E98D(9), 1630–1636. https://doi.org/10.1587/transinf.2014OPP0004.

Mountrakis G., Im J. & Ogole C., 2011. Support vector machines in remote sensing: A review. *ISPRS Journal of Photogrammetry and Remote Sensing*, 66(3), 247–259. https://doi.org/10.1016/j.isprsjprs.2010.11.001.

Rahmonov O., 2001. Pustynia Błędowska – fenomen krajobrazu. [in:] Rybak A., Wójcik A.J. & Woźnicka Z. (red.), *Dąbrowa Górnicza: monografia. Tom 1, Środowisko przyrodniczo-geograficzne*, Muzeum Miejskie „Sztygarka", Dąbrowa Górnicza, 293–317.

Rahmonow O., 1999. *Procesy zarastania Pustyni Błędowskiej*. Wydział Nauk o Ziemi, Uniwersytet Śląski, Sosnowiec.

Regionalna Dyrekcja Ochrony Środowiska w Krakowie, 2023. *Pustynia Błędowska*. https://www.gov.pl/web/rdos-krakow/pustynia-bledowska [access: 10.08.2024].

Van Anh T., Thi Le L., Nhu Hung N., Thanh Nghi L. & Hong Hanh T., 2021. Monitoring vegetation cover changes by Sentinel-1 radar images using random forest classification method. *Inżynieria Mineralna – Journal of the Polish Mineral Engineering Society*, 1(2), 441. https://doi.org/10.29227/IM-2021-02-41.

Zennaro F., Furlan E., Simeoni C., Torresan S., Aslan S., Critto A. & Marcomini A., 2021. Exploring machine learning potential for climate change risk assessment. *Earth-Science Reviews*, 220, 103752. https://doi.org/10.1016/J.EARSCIREV.2021.103752.